

This article was downloaded by:

On: 26 January 2011

Access details: *Access Details: Free Access*

Publisher *Taylor & Francis*

Informa Ltd Registered in England and Wales Registered Number: 1072954 Registered office: Mortimer House, 37-41 Mortimer Street, London W1T 3JH, UK



Liquid Crystals

Publication details, including instructions for authors and subscription information:

<http://www.informaworld.com/smpp/title~content=t713926090>

Structure analysis of side chain liquid crystal polymer films by means of electron microscopy

I. G. Voigt-martin^a; H. Durst^b

^a Institut für Physikalische Chemie der Universität Mainz, Jakob-Welder Weg 15, Mainz, F.R. Germany

^b Max-Planck-Institut für Polymerforschung, Mainz, F.R. Germany

To cite this Article Voigt-martin, I. G. and Durst, H.(1987) 'Structure analysis of side chain liquid crystal polymer films by means of electron microscopy', *Liquid Crystals*, 2: 5, 585 – 600

To link to this Article: DOI: 10.1080/02678298708086317

URL: <http://dx.doi.org/10.1080/02678298708086317>

PLEASE SCROLL DOWN FOR ARTICLE

Full terms and conditions of use: <http://www.informaworld.com/terms-and-conditions-of-access.pdf>

This article may be used for research, teaching and private study purposes. Any substantial or systematic reproduction, re-distribution, re-selling, loan or sub-licensing, systematic supply or distribution in any form to anyone is expressly forbidden.

The publisher does not give any warranty express or implied or make any representation that the contents will be complete or accurate or up to date. The accuracy of any instructions, formulae and drug doses should be independently verified with primary sources. The publisher shall not be liable for any loss, actions, claims, proceedings, demand or costs or damages whatsoever or howsoever caused arising directly or indirectly in connection with or arising out of the use of this material.

Structure analysis of side chain liquid crystal polymer films by means of electron microscopy

by I. G. VOIGT-MARTIN

Institut für Physikalische Chemie der Universität Mainz, Jakob-Welder Weg 15,
Mainz, F.R. Germany

and H. DURST

Max-Planck-Institut für Polymerforschung, Mainz, F.R. Germany

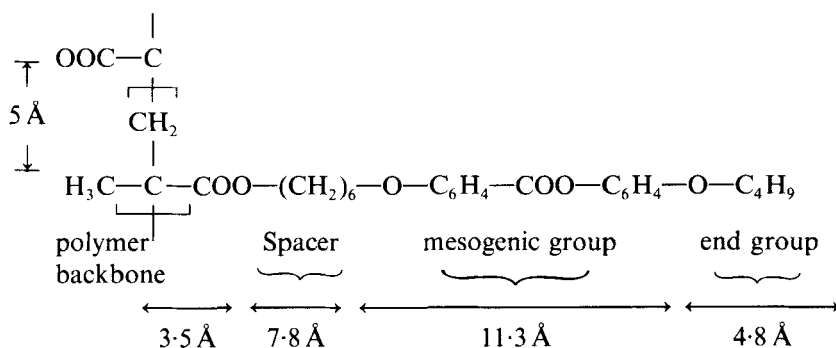
(Received 23 December 1986; accepted 9 May 1987)

Using the combined techniques of electron diffraction, bright and dark field electron microscopy as well as light microscopy, it has been possible to obtain detailed structural information about the arrangement of the smectic layers in a polymethacrylate side chain liquid crystal polymer with a biphenylester as the mesogenic group.

1. Introduction

1.1. Chemical constitution of the sample

The side chain liquid crystal polymer used in this work is a polymethacrylate with a mesogenic group in the side chain. It was synthesised by R. Zentel and has been described in detail elsewhere [1, 2]. The molecular structure of the sample is



The numbers indicate the length of the side chain in the extended all trans conformation of the chain. A photograph of a model depicting this molecule (part of the main chain with three complete side chains to the right and three incomplete side chains to the left) is shown in figure 1. According to both the model and to calculation, the length of the extended side chain is 27.4 Å.

2. Results

2.1. D.S.C. measurement

D.S.C. measurements of these samples (cf. figure 2) indicate three phase transitions, isotropic-nematic (386 K), nematic-smectic (383 K) and smectic-glass (300 K-320 K), as measured during heating and the same transitions 3 K lower as

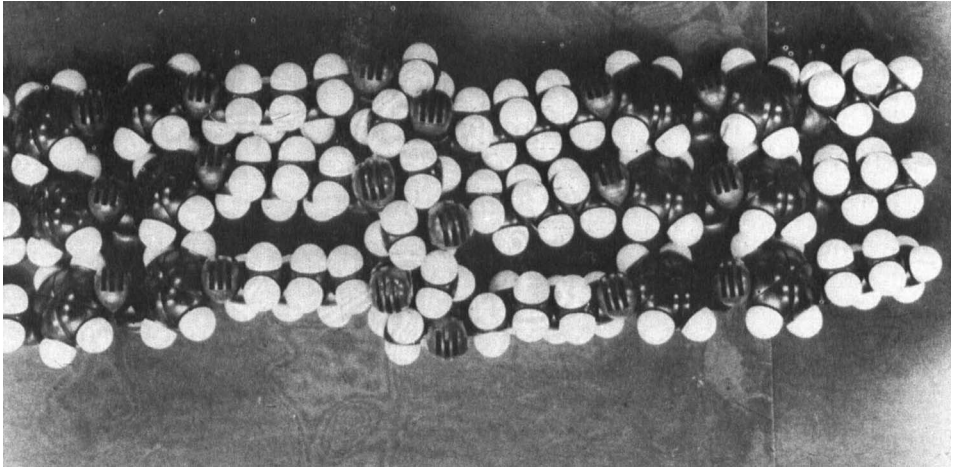


Figure 1. Model of the polymethacrylate side chain liquid crystal polymer with a biphenyl ester as the mesogenic group.

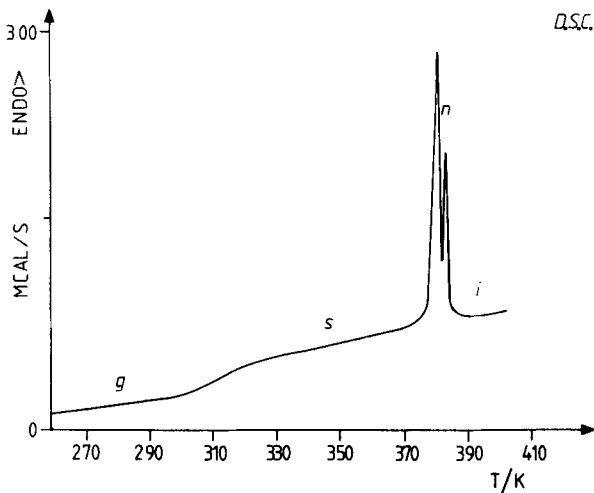


Figure 2. D.S.C. trace obtained from the polymethacrylate side chain liquid crystal with a biphenyl ester as the mesogenic group.

measured during cooling. Normally the transitions from isotropic to nematic and nematic to smectic are first order [3] and, on further cooling, the supercooled liquid crystal phase eventually forms a glass below T_g . It is well known that the phase behaviour of liquid crystal polymers depends strongly on three factors:

- (a) the size of the end group (6.8 Å);
- (b) the length of the spacer (6.8 Å);
- (c) the distance of the main chain between the side chains (5 Å).

For PMA side chain liquid crystal polymers it can be shown [4] that by replacing the butoxy end group (OC_4H_9) (6.8 Å) by a methoxy end group (OCH_3) (3.8 Å) (all other chemical constituents being equal), the nematic–smectic transition is suppressed.

2.2. Production of thin films

The production of thin films having a reproducible structure is not a trivial matter. The structure depends on film thickness, the amount of pre-orientation and the annealing temperature. The samples discussed here were always produced in an identical manner and always formed identical structures, as judged by light microscopy, electron microscopy and electron diffraction. The polymer, in 0.1 per cent chloroform solution, was pre-oriented by spreading on a water surface or by rotation in a spin coater. Subsequently it was annealed in the smectic phase close to the smectic–nematic transition (95°C for 2 hours) and subsequently cooled below the glass transition temperature. The thickness of the film can be judged by the interference colours. Thicker films were used for light microscopy whereas thin films were retained for electron microscopy. In both cases the samples were sandwiched between carbon films during annealing in order to produce identical and reproducible conditions.

2.3. Light microscopy

The light microscopical textures observed for these samples are identical to those which are typical for the smectic phase of low molar mass liquid crystals (cf. figure 3) [5]. These features are termed as bâtonnets, which coalesce to build up a focal conic texture. This texture has been observed for low molar mass materials in the smectic A, B and E phases. The molecular architecture for these is represented schematically in figure 4. Whereas all three phases have a layered structure, they are distinguished from one another by the packing within each layer. However in considering possible packing within the layers there is one important difference between the low molar mass liquid crystals and side chain liquid crystal polymers; namely, whereas the volume swept out by the small molecule during its motion is a cylinder (cf. figure 5(a)) that of the side chain liquid crystal polymer is a cone, since the side chain is pinned at one end by its position on the polymer backbone (cf. figure 5(b)); it is therefore



Figure 3. Light microscopy of the side chain liquid crystal with a biphenyl ester as the mesogenic group.




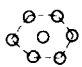

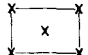
Phase Description	Layer Structure	Packing of molecules within Layers
S_A		 isotropic
S_B		 hexagonal
S_E		 orthorhombic

Figure 4. Schematic diagrams of smectic phases which give focal cone fan texture.

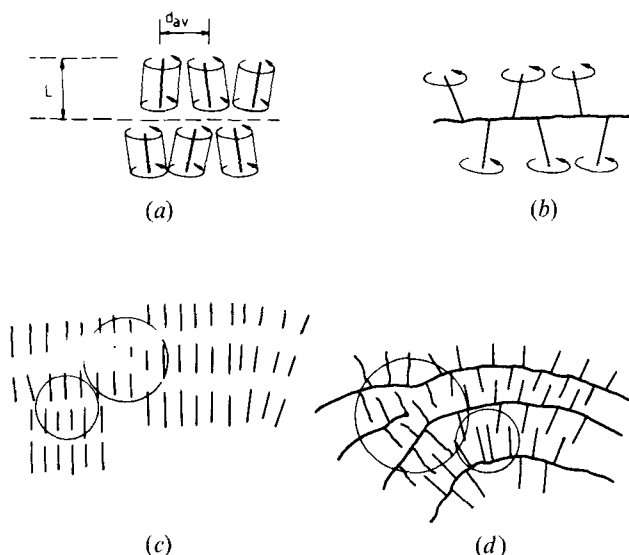


Figure 5. Possible molecular packing in liquid crystals. (a) Small molecule liquid crystal; (b) side chain liquid crystal polymer; (c) introduction of defects into structure of small molecule liquid crystals; (d) introduction of defects into structure of side chain liquid crystal polymer.

less mobile. Details regarding the packing will depend on the chemical constituents. The polymer backbone will also have a considerable influence on the defect structures which can arise. Whereas the low molar mass liquid crystals can form defect structures such as dislocations of fairly low energy (cf. figure 5(c)) the same defect may require considerable distortion of the polymer backbone (cf. figure 5(d)). This is expected to be the case for the side chain liquid crystal polymer under consideration. The details will however depend on the geometry involved; for example, in some polymers it is mandatory to introduce defects in order to alleviate stresses caused by undue distortion of the polymer backbone [6].

2.4. Surface replicas

Surface replicas used in electron microscopy provide information about the surface structure of a sample. They were obtained by shadowing the liquid crystal films obliquely with C/Pt (20°) and they were subsequently studied by electron microscopy without dissolving away the sample. A number of interesting features were observed at low magnification:

- (a) the films form surface steps (cf. figure 6(a));
- (b) some layers have irregular dark stripes (distance 2 μm) while others are structureless;
- (c) in regions where the film is torn, fibrils bridge the gap (cf. figure 6(b));
- (d) at intermediate magnifications it can be seen that the surfaces of the structureless regions are rougher than those containing the stripes (cf. figure 6(c)).

From the known shadowing angle and the length of the shadow at the edges of the films, it is easy to estimate the step height as being ~50–80 Å.

2.5. Transmission bright field and diffraction

In normal bright-field transmission, the now familiar stripes with a spacing in the micron range appear (cf. figure 7(a)), whereas in some regions there is no contrast.

It is difficult to obtain diffraction patterns from these samples because they are very beam sensitive. Certainly it is mandatory to use cryotechniques. The diffraction pattern from such samples is generally of the type typically observed from smectic phases (cf. figure 7(b)) showing three clear orders of sharp small angle diffraction maxima with very slight arcing and a broad oriented halo perpendicular to it at wide angles. The diffraction maxima were calibrated by evaporating TiCl directly onto the sample and the spacings

$$L_1 = 28.48 \text{ \AA}, \quad L_2 = 14.25 \text{ \AA}, \quad L_3 = 9.49 \text{ \AA},$$

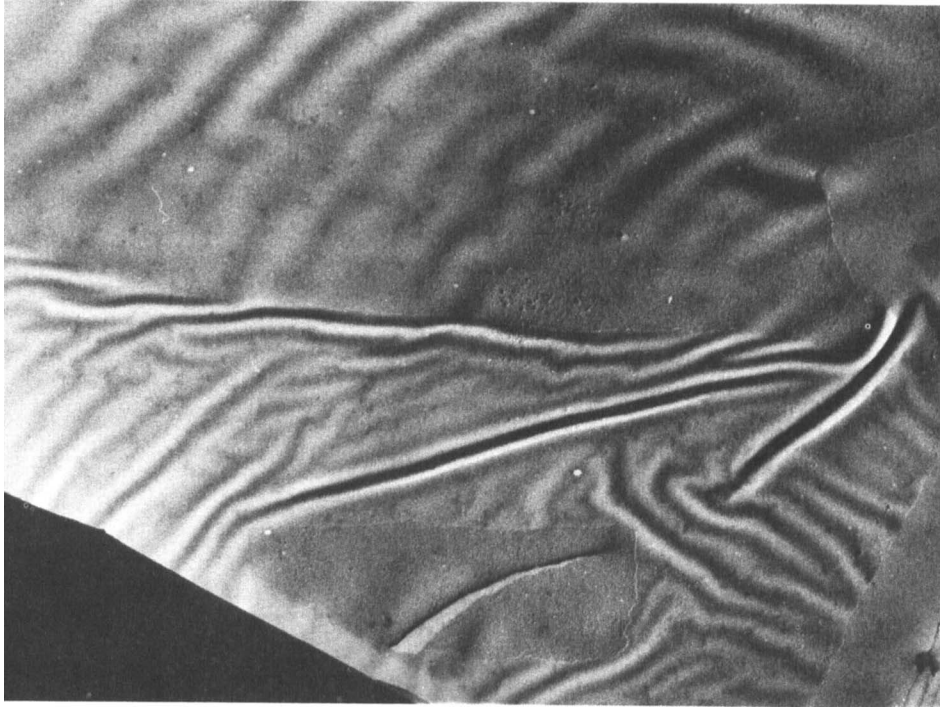
were evaluated. The average value of the wide angle spacing was about 4.5 Å. This indicates a smectic layer spacing of 28.48 Å with a second and third order diffraction maximum. In this case the side chains lie *in the plane* of the film. Occasionally a single crystal diffraction pattern is observed (cf. figure 8) with the spacings

$$d_1 = 4.17 \text{ \AA}, \quad d_2 = 3.82 \text{ \AA}, \quad d_3 = 2.47 \text{ \AA}, \quad d_4 = 2.26 \text{ \AA}, \\ d_5 = 2.07 \text{ \AA}, \quad d_6 = 1.88 \text{ \AA}, \quad d_7 = 2.23 \text{ \AA}.$$

Since the small angle spacings are missing from these diffraction patterns, it is clear that the side chains are *perpendicular to* the film. From the replicas we know that the film layers in these regions are about 50 Å thick, so that this packing occurs only in single layers. It should also be stressed that this is not a common occurrence and the usual situation is the one depicted in the first case, with smectic planes in the plane of the layers.

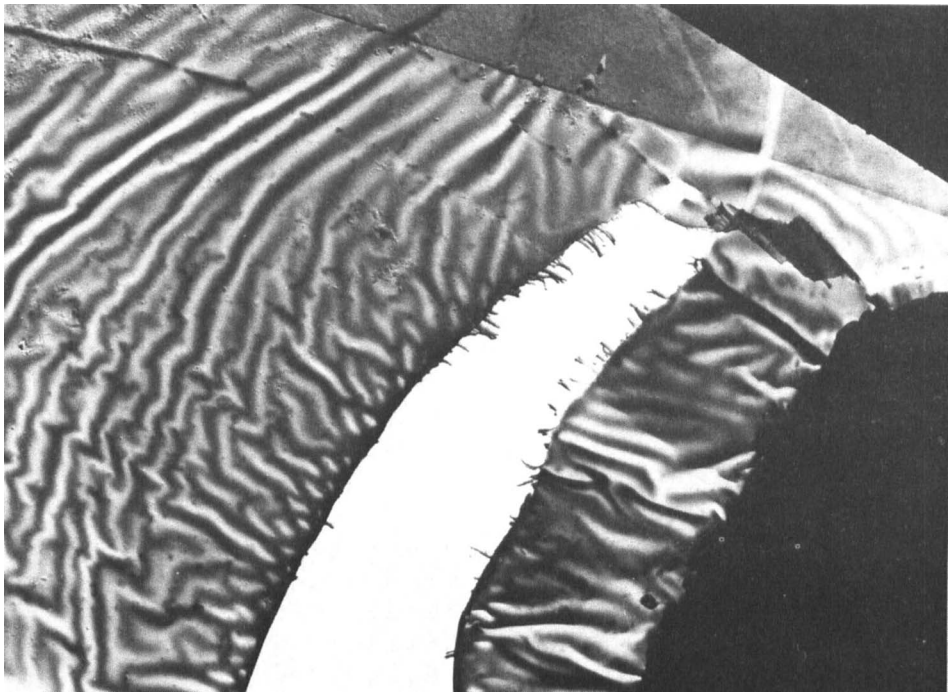
2.6. Transmission dark field

In order to determine the distribution of these smectic regions within the layers, dark field techniques were employed; in this technique only the beam diffracted into the small angle region is used to form an image. Consequently only those areas appear bright which gave rise to that particular diffraction maximum; in this case, it is the regions containing the smectic layers. The result is shown in figure 9 with the inset diffraction pattern in the correct orientation. It is clear that the areas giving rise to the



(a)

5 μm



(b)

5 μm

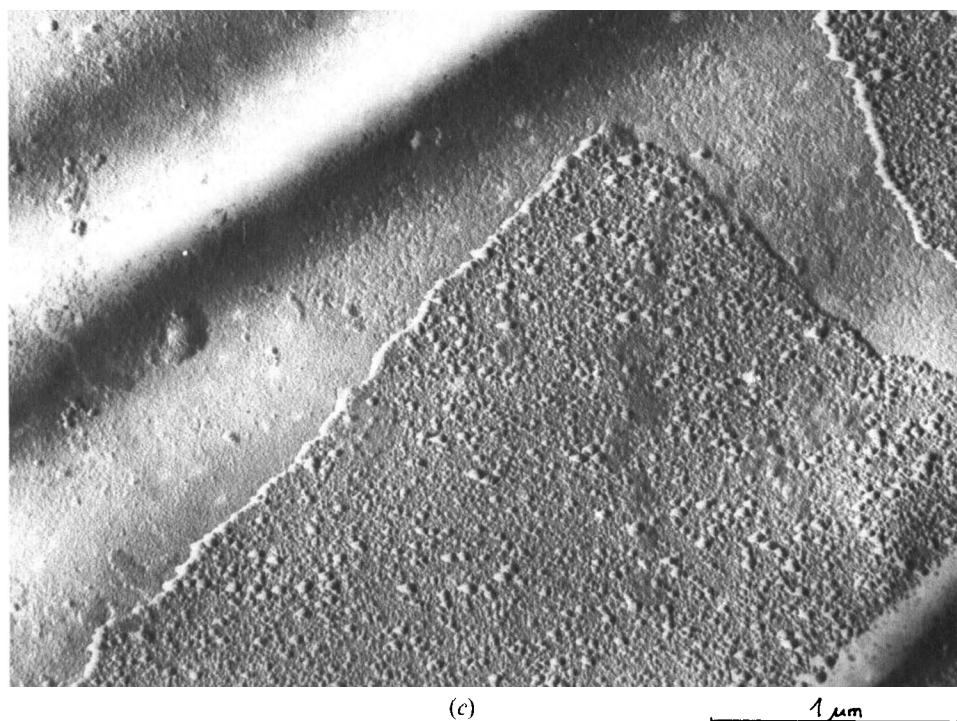


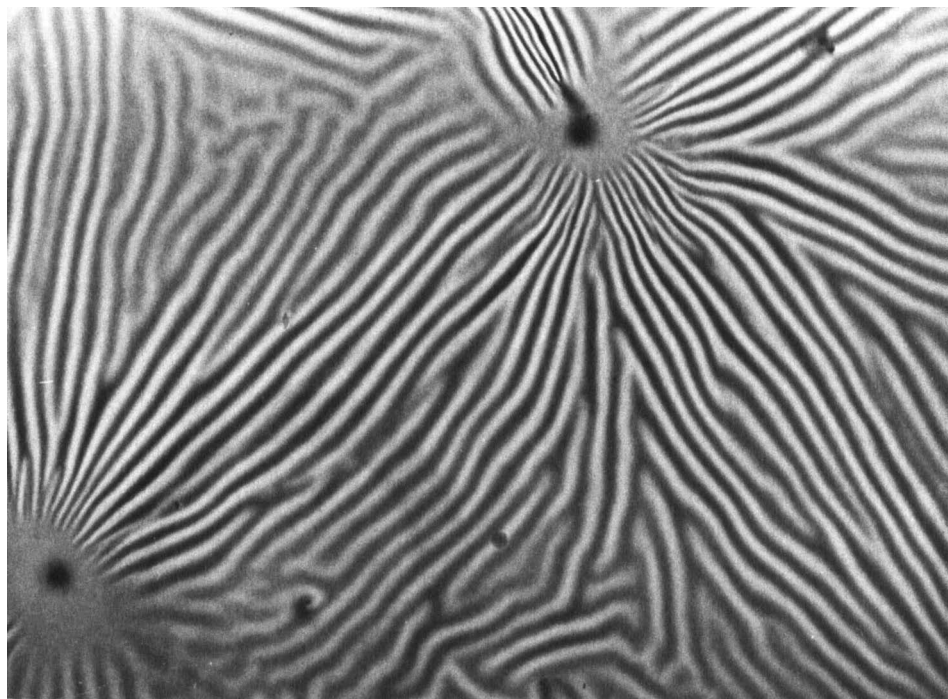
Figure 6. Replica of the side chain liquid crystal film showing (a) layered structures, (b) fibrils bridging a gap, (c) the different surface structures.

diffraction maxima are not spread over the whole sample but are distributed parallel to one another in elongated regions throughout the sample. The long dimension is several microns and the short dimension is $\sim 600 \text{ \AA}$. The correctly oriented diffraction pattern shows that the smectic layers are perpendicular to the long dimension; i.e. the side chains are parallel to the long dimension of the bright regions and the polymer backbone is perpendicular to it. From these micrographs it is impossible to deduce anything about the molecular orientation between these bright regions. The only thing which can definitely be claimed is that such regions do not contribute to the observed diffraction pattern. A dark field micrograph from the (rare) regions giving the single crystal diffraction pattern is indicated in figure 10.

3. Discussion of the results

It has been shown by replication that the thin films consist of three or four layers, about $50\text{--}80 \text{ \AA}$ thick. The layers seem to have a characteristic surface roughness; the rougher layers give rise to an orthorhombic diffraction pattern while the more generally observed smooth regions give rise to the typical smectic diffraction pattern, with three very sharp, slightly arced small angle maxima and a broad oriented halo perpendicular to it. The layer structures do not appear to be a phenomenon associated only with thin films. Figure 11 shows a surface replica obtained from a cryo-fractured bulk sample, which clearly shows terraces with a step height $\sim 40\text{--}50 \text{ \AA}$.

Before suggesting models which can account for the diffraction and dark field evidence, it will be necessary to understand the origin of the stripes, which are always



(a)

 $5\ \mu\text{m}$ 

(b)

Figure 7. (a) Bright field transmission micrograph. (b) Electron diffraction pattern of type A.

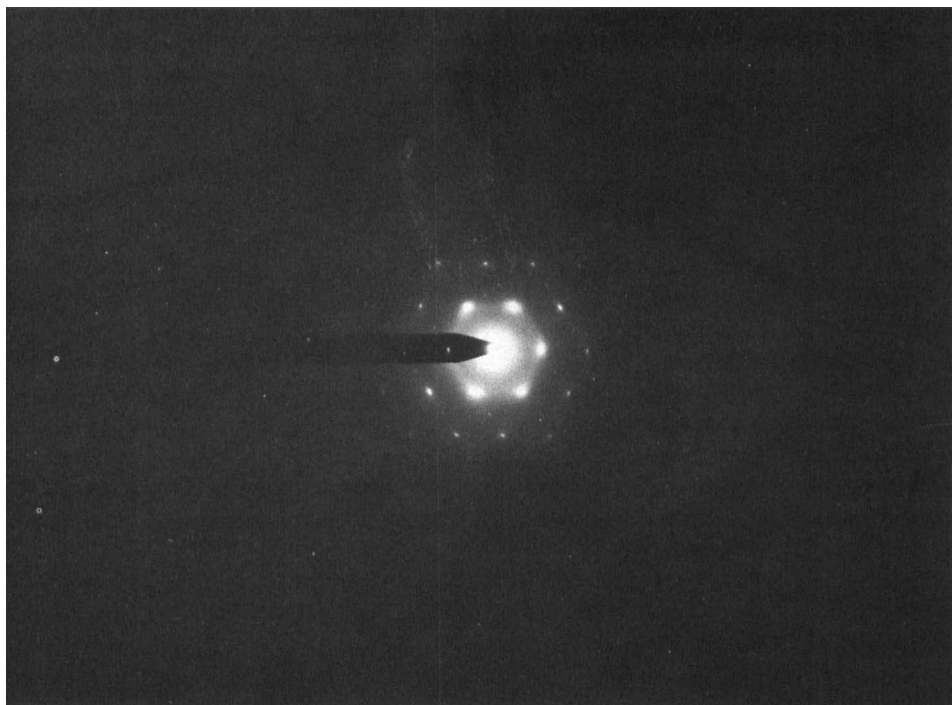


Figure 8. Electron diffraction pattern of type B (rarely observed).

observed in thicker films. At first sight, the stripes appear reminiscent of the banded structures described in several papers by Donald and Windle [7, 8] on the main chain liquid crystal polymers. Because such samples are very stable in the electron beam, these authors were able to obtain detailed dark field evidence from sections of the oriented halo obtained when the samples are sheared, and were able to show that the bands are associated with the serpentine path of the molecules in the shear direction. However, there are some important differences between the stripes observed in the side chain liquid crystal polymers and the bands observed in the main chain liquid crystal polymers. Our stripes were observed in identical positions in both bright and dark field. The bands were observed only in dark field and their position depended on the spatial frequencies used for microscopy. Thus the bands were clearly a diffraction effect. The stripes in these samples are a bright field phenomenon; the scattering regions observed in dark field are entirely unaffected by their presence. The origin of the stripes in these samples is therefore not immediately obvious; such features could result from scattering or diffraction contrast. Scattering contrast has two possible origins:

- (a) the presence of atoms with a higher atomic number: or
- (b) thickness undulations in the sample, causing multiple scattering and thus loss of electrons in the image.

Diffraction effects also give rise to fringes in specific situations:

- (c) the intensity varies as $[\sin^2(\pi ts)/(\pi s)^2]$ (i.e. it oscillates) in a wedge crystal of changing thickness t ; in this case s is the displacement of the Ewald sphere from the reciprocal lattice point g ; or

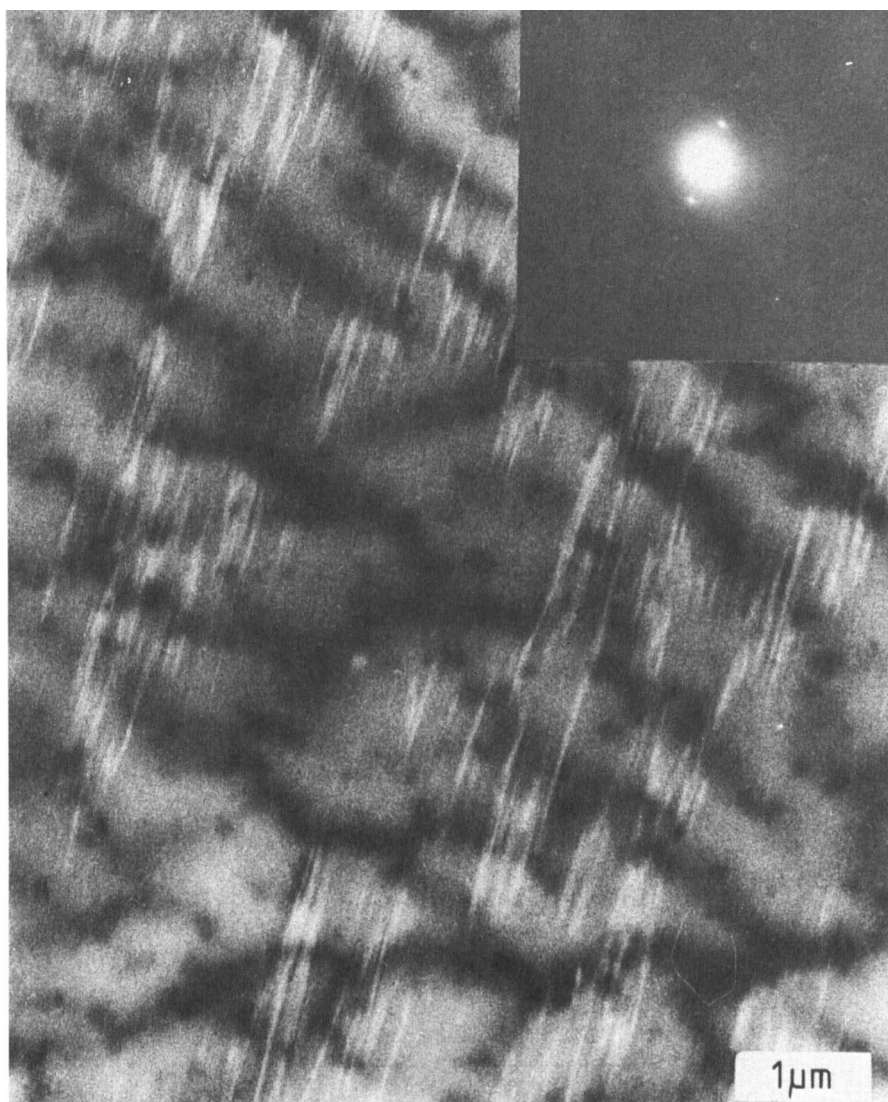


Figure 9. Dark field image from the side chain liquid crystal with an approximately oriented diffraction pattern.

(*d*) stacking faults cause fringes whose periodicity depends on the position of the fault with respect to the centre of the film.

Possibility (*a*) can be excluded because there are no heavy atoms in this sample which could be responsible for scattering of such magnitude. Thickness undulations (possibility (*b*)) should give rise to shadows when the platinum is evaporated on to the sample at a very oblique angle. Indeed, there are occasionally such indications, for example at positions A in figure 6(*b*); however the evidence is not very convincing in all regions. Possibilities (*c*) and (*d*) also remain, although diffraction fringes are actually calculated only for crystalline substances with three-dimensional order and not for liquid crystals, which are ordered only in one direction. However one thing

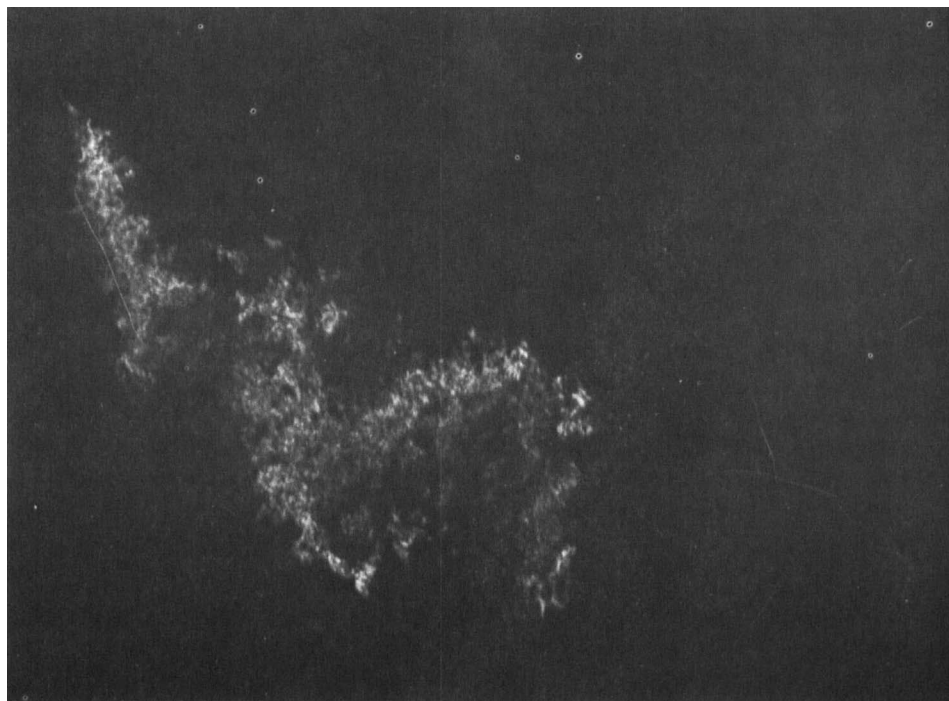


Figure 10. Dark field micrograph from a region giving rise to the orthorhombic diffraction pattern.

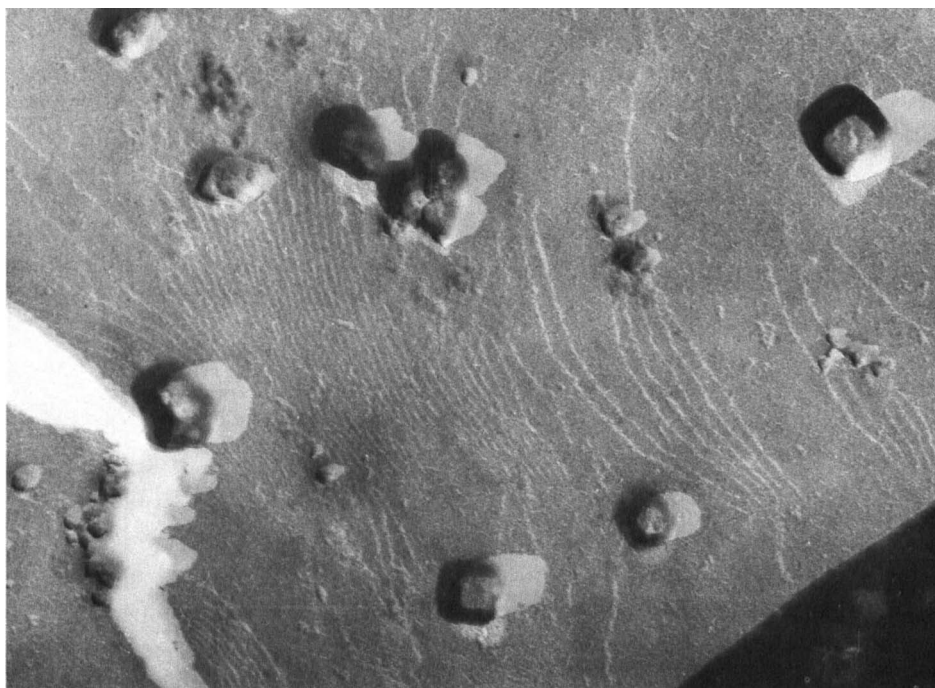
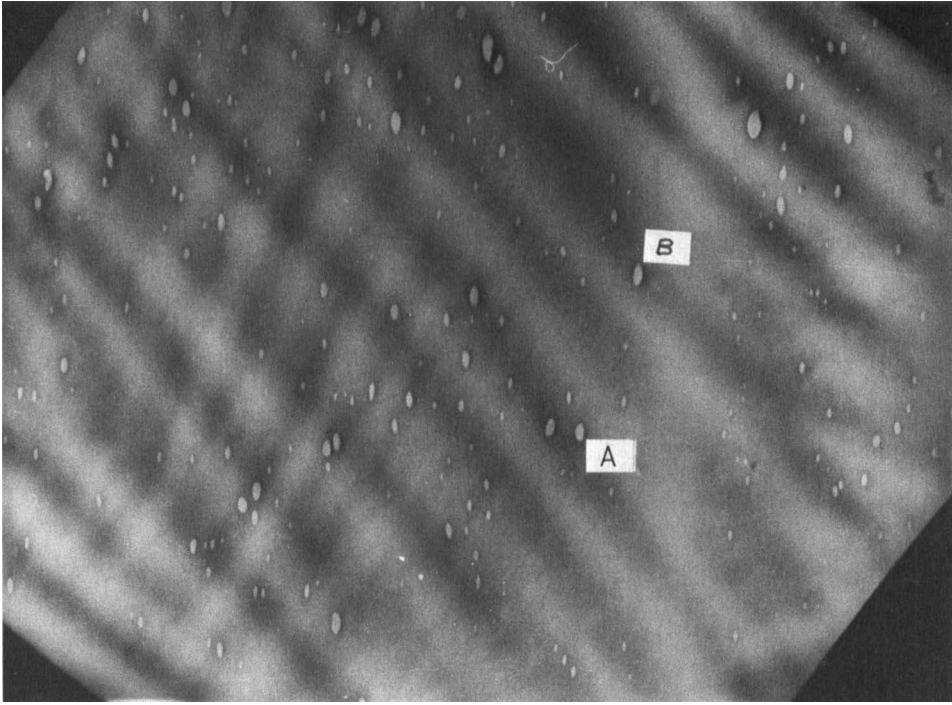
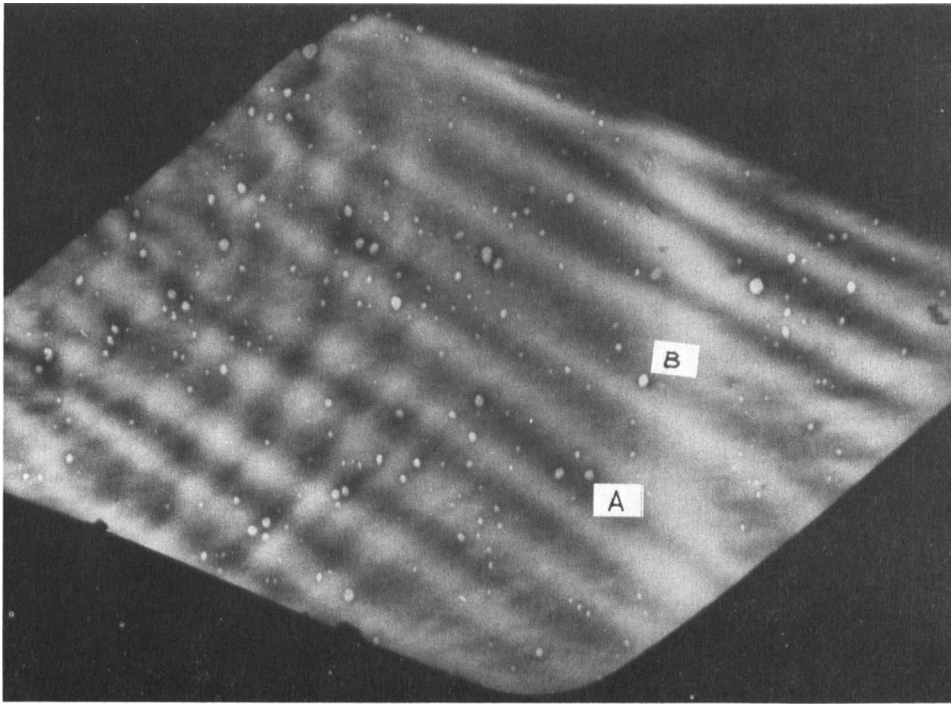


Figure 11. Surface replica from a cryo-fractured bulk specimen.



(a)



(b)

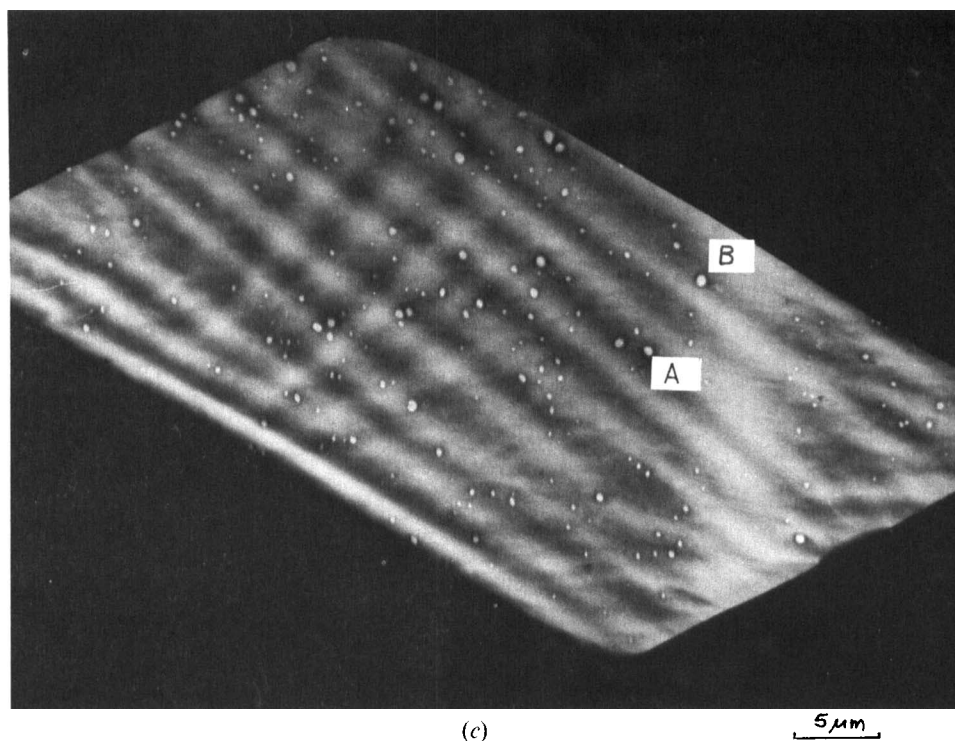


Figure 12. Series of tilt experiments to determine the origin of the stripes.

is common to all diffraction contrast; it moves its position on the sample when the sample is tilted. Figures 12(a), (b) and (c) show the result of tilting the sample by an angle of $\pm 60^\circ$; the stripes move closer together but *do not change their position* on the sample. In order to prove this, a specimen with holes was produced; the holes at A and B are marked on the sample at 0° tilt and at a tilt of $\pm 60^\circ$. The stripes remain on these holes and therefore move together in exactly the same ratio as the holes (this relationship is of course $(d/d \cos 60^\circ)$ if the tilt axis coincides with the stripe axis). This can be regarded as rather conclusive evidence that the position of the stripes in the sample is fixed and that they originate from thickness undulations which are, however, so gradual that they do not cause a shadow even at very low shadowing angles. The observation that the thick stripes are unaffected by dark field imaging and that the bright scattering regions are entirely unaffected by the positions of the stripes supports the conclusion that the stripes are not caused by diffraction contrast. Rather, they are thickness undulations created during flow; their frequency and width depend on the film thickness. They do not prevent or hinder formation of the smectic layer.

The smectic layers are evident in the diffraction pattern, obtained from almost all areas in the films (cf. figure 7(b)). Perpendicular to these are oriented halos arising from the side chains. In principle it is possible to envisage two possible arrangements for the structure (cf. figure 13(a), (b)). From the small angle spacing of 28.48 \AA it is clear that arrangement (b) is favoured in the thin film samples under consideration. The smectic layers show long range order, as indicated by the presence of the higher

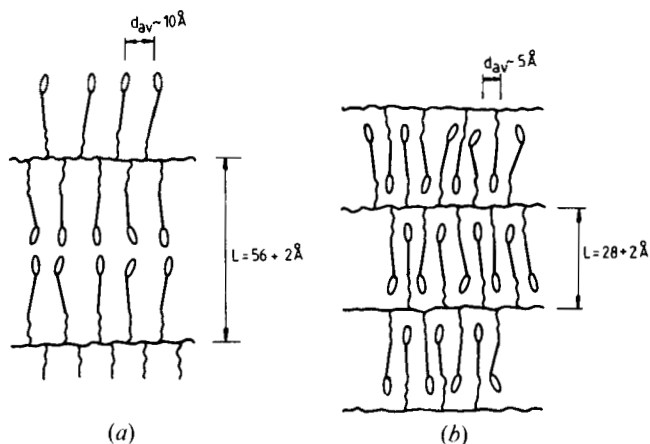


Figure 13. Schematic representation showing two idealized arrangements for macromolecules of the polymethacrylate side chain liquid crystal polymer.

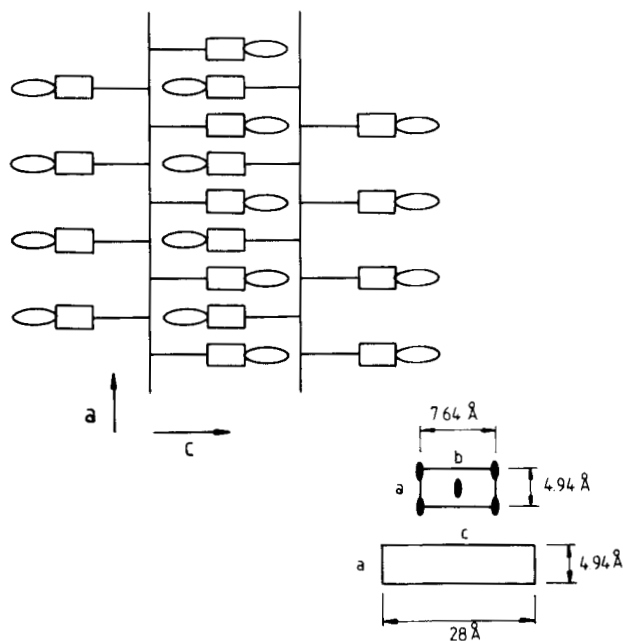


Figure 14. Ideal packing of side chains in a single layer which produces the orthorhombic diffraction pattern.

diffraction orders. The length of the extended side chain is 28 \AA and the end group is 4 \AA shorter than the extended spacer plus the carboxyl group, so that the distance between the smectic layers would be $(28 + 4) \text{ \AA}$ if the spacer were fully extended. The small angle spacing of 28.48 \AA therefore indicates that the spacer group is not in its fully extended planar all-trans conformation. The occasional appearance of a single crystal diffraction pattern suggests that in these cases the direction of view is along the side chains. Since the films causing these patterns are about 50 \AA , it would appear that these are monomolecular layers. The fortuitous view down the side chain makes it

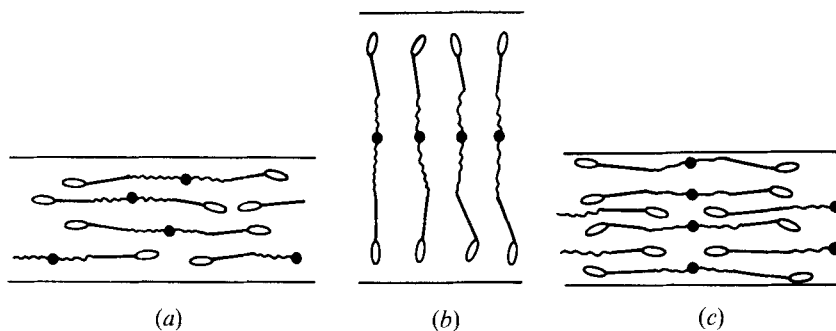


Figure 15. Schematic representation showing some possible arrangements for the side chains in thin films.

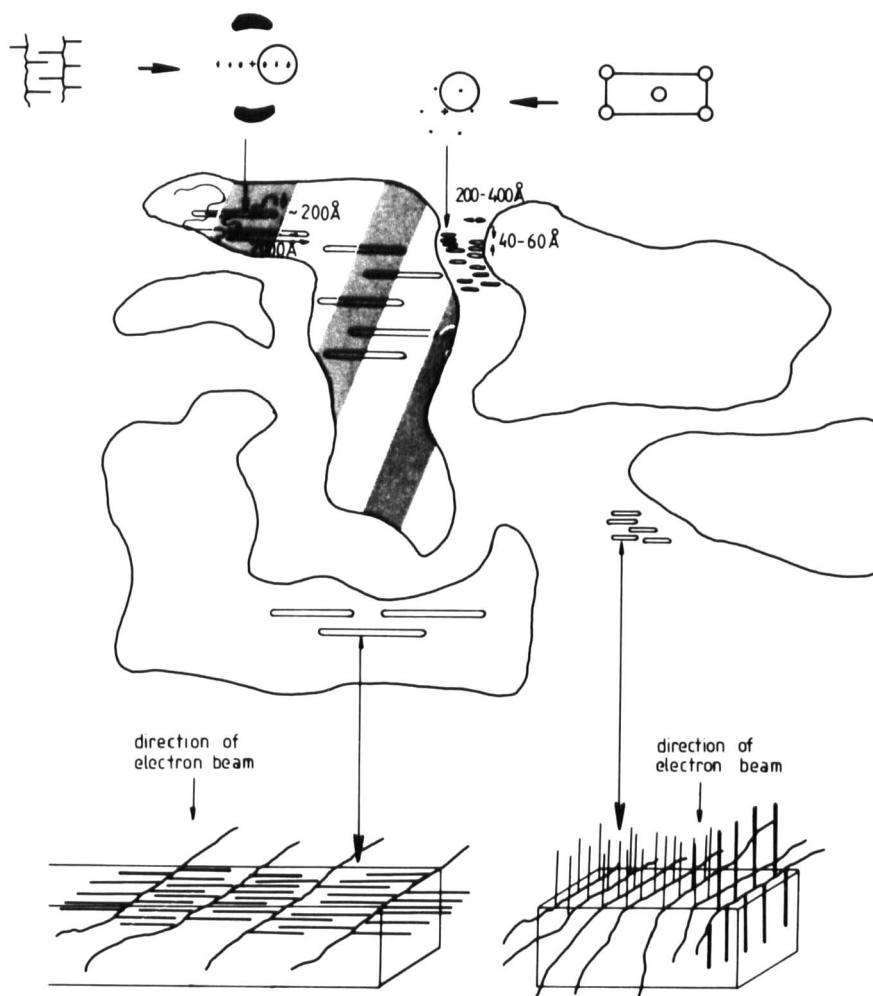


Figure 16. Structure of polymethacrylate side chain liquid crystal polymer films.

possible to estimate the packing of the side chains. On the assumption of an orthorhombic packing with the c axis in the side chain direction, the observed spacings can be indexed (cf. figure 14) as

$$\begin{aligned}d_1 &= 4.17 \text{ \AA} (110), & d_2 &= 3.82 \text{ \AA} (200), & d_3 &= 2.47 \text{ \AA} (020), \\d_4 &= 2.26 \text{ \AA} (410), & d_5 &= 2.07 \text{ \AA} (220), & d_6 &= 1.88 \text{ \AA} (400), \\d_7 &= 2.23 \text{ \AA} (310).\end{aligned}$$

Consequently two extreme situations have been observed (cf. figure 15), one in which the side chains are parallel to the film and one in which they are perpendicular, where the diffraction evidence favours arrangement (c).

The arrangement of molecules between elongated brightly scattering regions observed in the dark field micrographs is uncertain. It is possible that the layers are less perfectly arranged or that they are in a different orientation; in this case a series of tilting experiments should eventually give rise to small angle maxima from these intermediate regions. However, because of the extreme beam sensitivity of these samples and the enormous effort involved in order to obtain diffraction and dark field evidence, such experiments are not feasible.

The structure of the PMA side chain liquid crystal polymer films is represented in figure 16. There are large domains containing well-oriented regions with smectic layers parallel to the film surface. The regions are elongated ($\sim 2000 \text{ \AA}$) such that the side chains are parallel to the long edge and the main chain parallel to the short edge ($\sim 600 \text{ \AA}$). In addition to these large areas there are smaller regions in which the side chains are oriented perpendicular to the film surface and closely packed in an orthorhombic cell. It is expected that the size of the oriented regions is a function of annealing time, so that under favourable conditions the whole film would attain the orientation observed in the smectic regions.

The authors gratefully acknowledge the helpful comments and suggestions throughout this work by Dr. J. Wendorff and Dr. G. W. Schmidt. Furthermore we are indebted to the Deutsche Forschungsgemeinschaft for financial support.

References

- [1] ZENTEL, R., STROBL, G., and RINGSORF, H., 1985, *Macromolec.*, **18**, 960.
- [2] ZENTEL, R., 1980; Diplomarbeit University of Mainz.
- [3] FINKELMAN, H., and REHAGE, X., 1984, *Advances in Polymer Science* (Springer).
- [4] OHM, H., 1985, Dissertation, Mainz.
- [5] GRAY, G. W., and GOODBY, J. W., 1984, *Smectic Liquid Crystals* (Leonard Hill).
- [6] VOIGT-MARTIN, I. G., and DURST, H. (in preparation).
- [7] DONALD, A., and WINDLE, A. M., 1984, *J. Mat. Sci.*, **18**, 1143.
- [8] DONALD, A., and WINDLE, A. M., 1984, *J. Mat. Sci.*, **19**, 2035.